

On the use of dense seismic noise arrays for groundwater resources monitoring: results from a controlled infiltration experiment in a water catchment site

Stéphane Garambois*, Thomas Gaubert-Bastide, Camila Sanchez Trujillo, Christophe Voisin and Philippe Roux, Université Grenoble Alpes; Clarisse Bordes and Daniel Brito, Université de Pau et des Pays de l'Adour

Summary

Water resource management is a current crucial socio-economic issue that requires the development of high resolution monitoring techniques, including non-invasive hydrogeophysical methods. Among them, passive seismic interferometry offers an important potential in terms of characterization and above all of monitoring of the processes under study, and therefore those concerning environmental applications. Here, we propose to image and monitor with a dense passive seismic network the controlled groundwater changes artificially generated by infiltration ponds present at the urban water field supplying the Lyon Metropolis (France). Besides static imaging of the site, we could assess the hourly seismic velocity variations over 19 days during which two filling/drainage cycles of a water basin occur. The density of seismic stations offers the possibility to produce high resolution multi-frequency seismic velocity variation maps. They could highlight the implementation and hourly evolution of a hydraulic dome, which should act as a bulwark which should limit river/water table exchanges in case of pollution.

Introduction

The characterization and temporal monitoring of geological reservoirs is necessary for a very large number of Earth processes, and particularly those affecting the management of natural resources (groundwater, geothermal energy, gas storage, oil and gas resources) and natural hazards (volcanoes, earthquakes, landslides). For water resources management, it is common to use active methods but continuous monitoring is difficult to implement due to actual costs of maintaining the operation. Passive seismic methods, such as ambient noise cross-correlation, use stand-alone recording stations and benefits from continuous seismic noise sources that allow to study the seismic wavefield and to analyze its variations over time. It is based on the principle that the cross-correlation of two seismic noise records acquired by two sensors provides the Earth response to perturbations between the two sensors, the Green's function, if noise sources are isotropic. This methodology paved the way for the possibility of continuous temporal monitoring of Green's functions and particularly to track very fine seismic velocity variations related to any changes of the Earth properties.

Focusing on fluid flows, this approach was successfully used at various scales, for example to observe weak water table variations on the Merapi volcano (Sens-

Schönfelder et al., 2006), fluid flows during volcano eruptions (Breguier et al., 2011; Takano et al., 2020) or in various subsurface environmental processes (Larose et al., 2015 for a review). For groundwater monitoring, Lecocq et al. (2017) and Clements and Denolle (2018) used diffuse coda waves at large scale and for long times series, while Voisin et al. (2016) and Garambois et al. (2019) took benefit from the ballistic properties of direct surface waves. However, all these studies were performed with a sparse number of stations, which limited the possibility to precisely locate the velocity variations related to groundwater changes, although Clements and Denolle (2008) could regionalize the information and compare them with GPS data.

We propose here to investigate the capacity of using a dense seismic network to regionalize the groundwater changes generated by the filling/drainage of a water retention basin. Indeed, these cycles aims at creating a hydraulic dome whose spatial and time evolutions are expected to be large and are a crucial information in terms of water management of this operating site, due to potential pollution issues.

Data acquisition and processing

The Crépieux-Charmy water withdrawal site is a complex system which supplies 87% of tap water for the nearby Lyon metropolitan area (France, 1.4 Million of inhabitants). Located in the vicinity of a highly urbanized

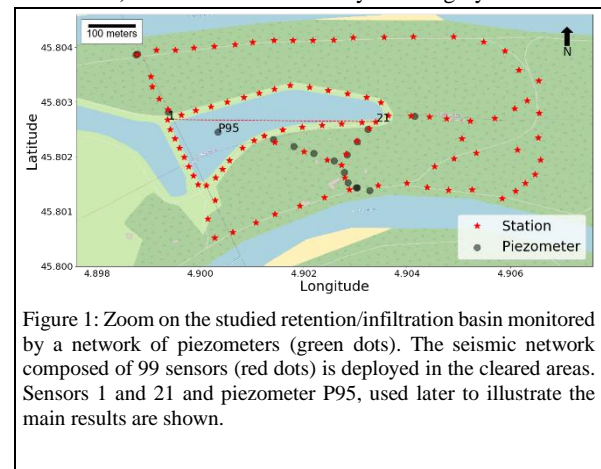


Figure 1: Zoom on the studied retention/infiltration basin monitored by a network of piezometers (green dots). The seismic network composed of 99 sensors (red dots) is deployed in the cleared areas. Sensors 1 and 21 and piezometer P95, used later to illustrate the main results are shown.

area and surrounded by rivers and canals, this strategic area is very sensitive to pollution risks, especially from rivers. In

Use of a dense seismic network for groundwater monitoring

order to protect the groundwater from river pollution, 12 infiltration ponds have been installed around the pumping areas in order to maintain the groundwater level and to artificially create a hydraulic dome by filling these basins.

On a smaller scale, basin 5.2 located near the Miribel

components were rotated according to the azimuth of the considered path. The CCs are then stacked over 10 minutes.

These calculations resulted in 3C correlograms for all station pairs, as illustrated for the station pair 1-21 for the TT

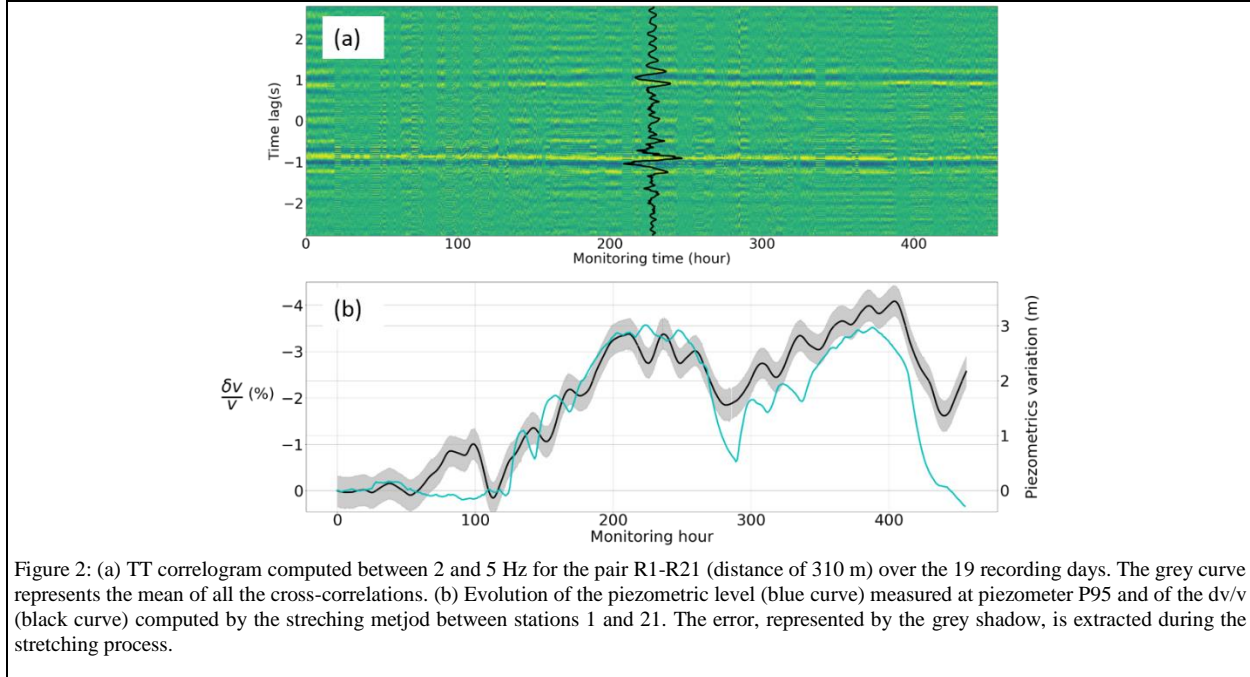


Figure 2: (a) TT correlogram computed between 2 and 5 Hz for the pair R1-R21 (distance of 310 m) over the 19 recording days. The grey curve represents the mean of all the cross-correlations. (b) Evolution of the piezometric level (blue curve) measured at piezometer P95 and of the $\frac{\delta v}{v}$ (black curve) computed by the stretching method between stations 1 and 21. The error, represented by the grey shadow, is extracted during the stretching process.

canal to the north has been designed to compensate for the effects of pumping on the water table but also modify the direction of the water flows, which naturally goes from the river towards the groundwater, by creating a hydraulic bulwark. Preliminary seismic noise studies combining data acquisition with a limited number of sensors and a numerical poroelastic approach (Garambois, 2019) showed the linear response of seismic ballistic velocity variations to the groundwater table. To regionalize with high spatial resolution the evolution of the artificially generated groundwater variations by basin infiltration, 99 seismic Fairfield 3C nodes have been deployed during 19 days around the basin infiltration basin (Figure 1). During this period, two infiltration cycles were performed.

The global workflow designed to compute reliable dynamic tomographic maps of velocity variations and a static imaging of the site is based on the cross-correlation (CC) of ambient noise for each station pair. The density of the network allowed to verify the location and stability of the noise sources via a beamforming approach. Then, we could compute the diagonal elements of the 4851 CCs every minute, i.e. the transverse (TT), Radial (RR) and Vertical (ZZ) one. For this, the original signals were whitened on a daily basis in the 1-20 Hz band and the original horizontal

component displayed in Figure 2 (a). It shows very stable symmetric events with a dominant wave arriving around 0.8 s, corresponding to an apparent velocity of roughly 400 m/s. It must be noted that the large number of available raypaths with a wide range of distance and the use of the 3 components helped us to clearly identify the different surface waves, notably by assessing their average phase dispersion curves. In addition, we could also assess the Vs 3D model of the site using a tomography of the group velocity curves. This study help us to identify the dominant wave of the TT component as the fundamental mode of the Love wave while the fundamental Rayleigh mode dominates the two other components.

In a second step, the velocity variations ($\frac{\delta v}{v}$) have been estimated from the TT component using a stretching technique (Sens-Schönfelder et al., 2006) focusing on the Love wave. The results are illustrated in Figure 2 (b) for the same station pair and compared with water table variations measured in piezometer P95 located along the considered raypath. The two curves are overall perfectly anti-correlated as explained by Garambois et al. (2019), who quantitatively related water saturation variations with surface wave velocity variations through a poroelastic. In particular, their linear relationship between $\frac{\delta v}{v}$ and water table variation (1 % = 1m), based on Rayleigh wave analysis, appears still

Use of a dense seismic network for groundwater monitoring

roughly valid, although here Love waves are considered. Small discrepancies exist and may come from the hazardous comparison between a local measurement performed in a well (piezometer) with an integrated one (along a path). This is especially true here where the basin filling is done in order to create large spatial gradients of the water table. Consequently, the high resolution imaging that tomography can bring us will allow us to better discuss these points.

Regionalization of the groundwater evolution

The regionalization of the velocity variations has been performed through a tomography process based on the (straight) ray theory approach of Barmin (2001). For this, all the 4851 dv/v measurements are considered in an iterative inversion process, where the rays exhibiting large RMS error greater than 70 % at a given iteration are suppressed for the following iteration. The process has been stopped after 3 iterations. We used a 44×22 roughly rectangular grid with a square mesh of size 19.9 m. A regularization spatial Gaussian term is used with a correlation length of 50 m and a smoothing strength of 0.05. A results of the process is shown Figure 3 at the monitoring hour 210. It shows the map of the dv/v variation relative to the beginning of the experiment. This image shows a strong homogeneity with a maximum of variations in the southern sector of the lake, slightly east of the filling point. We also see fairly moderate values within the basin as well as a north-south variation. The eastern part of the exploration area remains rather static with weak dv/v variations. The RMS error appears rather homogeneous on the whole grid, lower than 0.15. Only a few very sparse grid points show a larger error. At the final iteration, i.e. after removal of raypaths with large RMS, the ray density (Figure 3 (b)) remains very good with some cells illuminated by more than 150 rays, while on average, there is a density of 90 rays per cell, except on the edges of the grid.

This regionalization approach allows to track the hourly evolution of the velocity variations through time, although a better time resolution of 10 mn could have been achieved. A movie can thus be generated, from which critical times can be extracted. We have isolated in Figure 4 the maps obtained at four key moments representative of the first basin infiltration cycle. To facilitate its reading, we have placed in the center of this figure the continuous variations of the water table level measured at the level of the piezometer near the point of injection as well as the key moments (red stars). It highlights the build-up of a negative dv/v from 124 h which culminates at 225h, in agreement with measured water table variations. At this time, well-localized patches are visible within the basin, forming what looks like a dome stretched in the direction of the basin. Outside of the basin, smaller negative velocity variations can also be detected. Then the variations decrease slightly in value during the drainage cycle. Note that the second filling

cycle show almost the same information, except that at the end of the experiment, the system is not coming back the initial one in some areas. This surprising observation, could be linked to the presence of the second basin to the west,

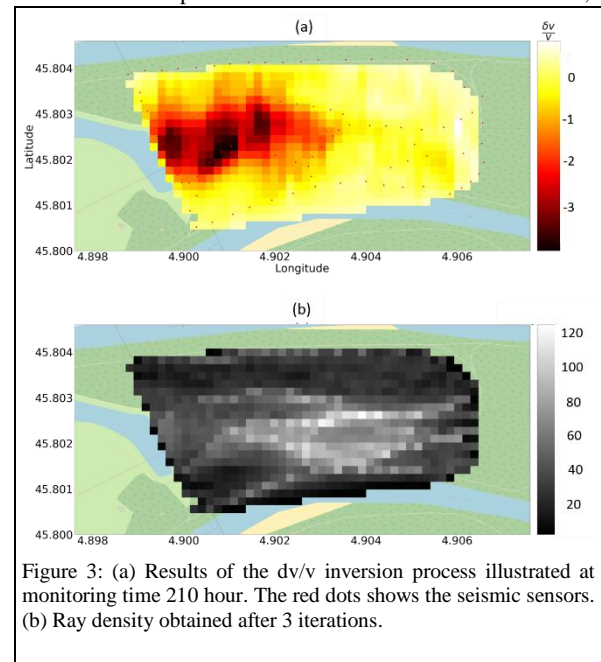


Figure 3: (a) Results of the dv/v inversion process illustrated at monitoring time 210 hour. The red dots shows the seismic sensors. (b) Ray density obtained after 3 iterations.

which was operating at the time of the experiment as well to the exchanges between rivers.

The presence of an array of piezometers around the basin, although sparse, allowed a more detailed spatial comparison between the groundwater variations locally measured and the tomographic dv/v results. In addition to a very good consistency between the two approaches, this comparative study clearly shows the advantage of using the seismic network for the reconstruction of the hydraulic dome. Indeed, the high tomographic resolution provided by the seismic network clearly shows the location of the apex and gradient of the dome, which is difficult for the piezometric approach, due to a low spatial sampling, especially in the northern and central parts of the site.

Conclusions

The use of a dense seismic network shows that passive seismic interferometry is able to image strong spatial gradients of the groundwater level and their evolution over time. The use of 3C sensors provides us with a better view of the wavefield studied. Beside this, a high resolution 3D Vs image of the site can be derived from the group velocity dispersion curve inversion. It allows us to better understand the geological variability of the sediments, which is an important information when water flow models are considered. This information also allows us to better take

Use of a dense seismic network for groundwater monitoring

into account the frequency variability of the seismic monitoring response, by calculating more precisely the sensitivity kernels of the considered ballistic waves. This could allow adding depth information to the 2D variations already available.

To sum up, there is a strong potential of using dense seismic networks to monitor large groundwater variations with a high resolution. In the near future, the use of fiber-optic measurements, with their impressive spatial resolution, will certainly increase the efficiency to manage water resource.

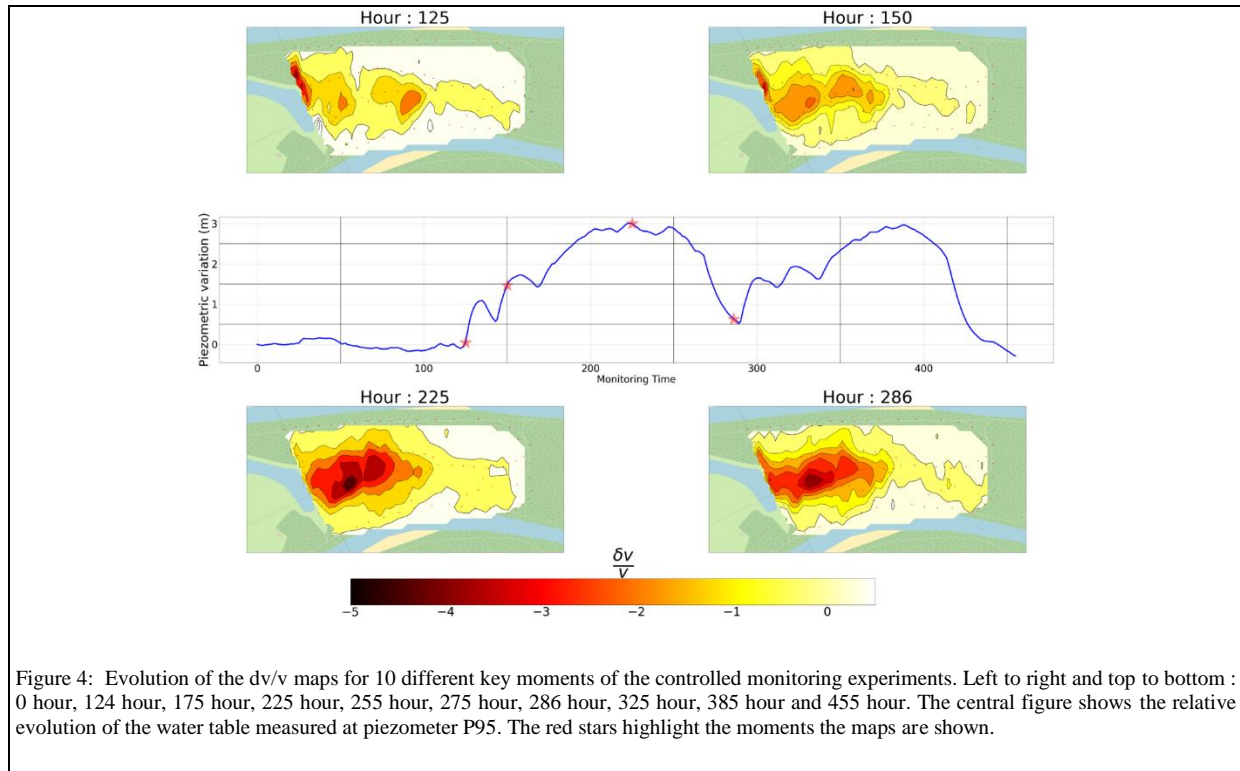


Figure 4: Evolution of the $\delta v/v$ maps for 10 different key moments of the controlled monitoring experiments. Left to right and top to bottom : 0 hour, 124 hour, 175 hour, 225 hour, 255 hour, 275 hour, 286 hour, 325 hour, 385 hour and 455 hour. The central figure shows the relative evolution of the water table measured at piezometer P95. The red stars highlight the moments the maps are shown.

Acknowledgments

The authors thank Laurent Oxarango and Isaam Seiffeidine for access to the piezometric data and the “Plateforme de recherche de Crépieux-Charmy” for granting access and support for the experiments. The study was performed thanks to the RESOLVE Grant (IRS-UGA).